Journal of the European Ceramic Society **12** (1993) 87–96

Relaxation Dispersion of Ionic Conductivity in a $Zr_{0.85}Ca_{0.15}O_{1.85}$ Single Crystal

A. Orliukas, P. Bohac,* K. Sasaki & L. Gauckler

Nichtmetallische Werkstoffe, ETH Zürich, CH-8092 Zürich, Switzerland

(Received 7 August 1992; revised version received 12 February 1993; accepted 17 February 1993)

Abstract

The dynamic behavior of the oxygen ion conductivity of a cubic $Zr_{0.85}Ca_{0.15}O_{1.85}$ single crystal has been investigated with AC impedance spectroscopy and a dynamic pulse method as a function of both temperature and frequency between 450 and 1200 K and 20 and 10^8 Hz. This is the frequency–temperature range where the relaxation dispersion of the ionic conductivity can be observed. From the temperature dependence of the relaxation frequency, the diffusion coefficient and the mobility of oxygen vacancies were determined. In the entire temperature range investigated, the temperature dependence of the ionic conductivity of a $Zr_{0.85}Ca_{0.15}O_{1.85}$ single crystal arises exclusively from the temperature dependence of the mobility of oxygen vacancies, the concentration of which remains constant with temperature and is equal to the concentration of all extrinsic oxygen vacancies created by calcia stabilizing. No transition in the Arrhenius plot of the ionic conductivity due to a gradual dissociation of oxygen vacancy–defect cation associates, as proposed in the literature, has been observed. A simple model for the temperature dependence of the ionic conductivity of solid electrolytes in terms of the parallel and serial combination of RC-elements is given.

Das dynamische Verhalten der Sauerstoffionenleitfähigkeit eines kubischen $Zr_{0.85}Ca_{0.15}O_{1.85}$ Einkristalles wurde mit der Impedanzspektroskopie sowie mit einer dynamischen Pulsmethode als Funktion der Temperatur und Frequenz zwischen 450 und 1200 K und 20 und 10^8 Hz untersucht. Das ist der Frequenz- und Temperaturbereich in welchem die Relaxationsdispersion der Ionenleitfähigkeit beobachtet werden kann. Aus der Temperaturabhängigkeit der Relaxationsfrequenz wurden der Diffusionskoeffizient und die Beweglichkeit der Sauerstoffleerstellen bestimmt. Im gesamten untersuchten Temperaturbereich entsteht die Temperaturabhängigkeit der Ionenleitfähigkeit des $Zr_{0.85}Ca_{0.15}O_{1.85}$ Einkristalles ausschlielich infolge der Temperaturabhängigkeit der Beweglichkeit der Sauerstoffleerstellen, deren Konzentration mit Temperatur konstant bleibt und gleich der Konzentration aller extrinsischer Sauerstoffleerstellen ist, die durch die Stabilisierung mit Calciumoxid entstanden sind. Es wurde kein Übergang in der Arrheniuskurve der Ionenleitfähigkeit infolge einer allmählichen Dissoziation von Assoziationskomplexen zwischen den Sauerstoffleerstellen und Defektkationen beobachtet, wie es in der Literatur vorgeschlagen ist. Die Temperaturabhängigkeit der Ionenleitfähigkeit der Festelektrolyte läßt sich mit einem einfachen Modell als eine Kombination von parallel und in Serie geschalteten RC-Elementen beschreiben.

Le comportement dynamique de la conductibilité ionique de l'oxygène dans un monocristal de $Zr_{0.85}Ca_{0.15}O_{1.85}$ cubique a été étudié par spectroscopie d'impédance complexe et par une méthode de pulsion dynamique, en fonction de la température et de la fréquence, entre 450 et 1800 K et 20 et 10^8 Hz. Ceci correspond au domaine de températures et de fréquences dans lequel la dispersion de la relaxation de la conductibilité ionique peut être observée. Le coefficient de diffusion et la mobilité des vacances d'oxygène ont été déterminés à partir de la variation de la fréquence de relaxation en fonction de la température. Dans tout le domaine des températures considerées, la variation de la conductibilité ionique des monocristaux de $Zr_{0.85}Ca_{0.15}O_{1.85}$ en fonction de la température provient exclusivement de la dépendance de la mobilité des vacances d'oxygène en fonction de la température. La concentration de ces vacances d'oxygène reste constante en fonction de la température et est égale à la concentration de toutes les vacances extrinsèques créees par le dopage à l'oxyde de calcium. Contrairement à ce qui a été proposé dans la litérature, nous n'avons observé, dans

* To whom correspondence should be addressed.

Journal of the European Ceramic Society 0955-2219/93/$6.00

le graphe d'Arrhenius, aucune transition de la conductibilité ionique, qui serait causée par une dissociation graduelle des associés 'vacances d'oxygène–défauts de cations'. La variation de la conductibilité ionique d'électrolytes solides en fonction de la température peut être décrite à l'aide d'un modèle simple basé sur la combinaison en paralléle et en série d'eléments RC.

1 Introduction

High oxygen ion mobilities with transference numbers for oxygen ions greater than 0·99 have been found for cubic zirconia solid solutions stabilized by substitution of di- or trivalent cations.[1-8] Today, zirconia-based materials are used for a variety of technical applications, namely as solid electrolytes in high-temperature fuel cells, water electrolyzers and electrochemical oxygen pumps, as well as for oxygen sensors and high-temperature heating elements. In spite of the extensive research directed toward the electrical properties of stabilized zirconias, the understanding of the nature of the charge transport process in these materials still remains incomplete and contradictory.[9-22]

To explain both the bend sometimes occurring in the Arrhenius curve ($\log \sigma T$ versus $1/T$) and the decrease of the ionic conductivity which has been found at high stabilizer concentrations, Hohnke[9] proposed that immobile associated complexes are partially formed between oxygen vacancies and oppositely charged cationic defects. For the association reaction an equilibrium mass action constant, $K = \exp(-\Delta G_A/RT)$, can be derived. The amount of free charge carriers available for migration depends on the content of stabilizer as well as on temperature. Since the dissociation of defect pairs requires an additional energy compared with the simple migration of 'free' oxygen vacancies, a higher conduction activation energy would be obtained at lower temperatures than at elevated temperatures at which all associates are already thermally dissociated.[9-12] A simple model based on the effective concentration of 'free' oxygen vacancies was proposed by Subbarao & Ramakrishnan.[13] The change in the activation energy between a low-temperature region, where vacancies are assumed to be bound to dopant cations, and a high-temperature region, where vacancies are assumed to be freely mobile, has been observed even in transparent single crystals of yttria-stabilized zirconia.[14-15]

On the other hand, it was shown already in 1981 in the study by Catlow[16] that if quasi-chemical equilibrium is assumed, the concentration of dissociated mobile oxygen vacancies would also increase as the content of stabilizer is raised. He claimed that at high stabilizer contents an increasing number of defect clusters strongly reduces the vacancy mobility. In the model of Abelard & Baumard[17] the frequency dispersion of dielectric bulk properties has been attributed to interactions between hopping oxygen vacancies and the randomly distributed network of stabilizer cations. The nonequivalent heights of energy barriers opposing the oxygen vacancy migration lead to a statistical, Gaussian distribution of the jump frequencies related to the time constant for the charge transport process. From the dielectric response, a 'transition frequency' has been determined, the activation energy of which remains constant with temperature and is equal to that of the electrical conductivity itself. Ananthapadmanabhan *et al.*[18] have found that even a partial replacement of ZrO_2 by CeO_2 decreases the ionic conductivity of yttria-stabilized zirconia because of an increased impedance to the motion of oxygen vacancies caused by an increased lattice scattering due to the differences in the size of the Zr and Ce ions.

In their general approach for solid electrolytes, Nowick *et al.*[19] distinguish three stages for the ionic conductivity as function of temperature:

(I) At rather high temperatures, usually above 0·5 $T_{melting}$, an intrinsic range of thermally activated defects (stage I) can be observed. The rather high activation energy for conduction in stage I consists of both the energy required for defect formation and the energy for defect migration.

(II) In the extrinsic dissociated range (stage II) occurring at medium temperatures, the relatively low concentration of intrinsic defects can be neglected but all extrinsic defects created by doping are mobile and available for conduction. The activation energy for conduction corresponds merely to the activation energy for the migration of extrinsic defects.

(III) In the extrinsic associated range (stage III), which can be observed at low temperatures, only a certain fraction of extrinsic defects has sufficient energy to overcome the energy barrier for migration. In addition to the migration energy, the activation energy for conduction includes also a substantial contribution from the dissociation energy of defect complexes.

According to this model, on decreasing the temperature, a first bend in the Arrhenius curve of ionic conductivity occurs to lower activation energy from stage I to stage II, in the temperature region where the concentration of the thermally created intrinsic defects is comparable with the concentration of the

impurity controlled extrinsic defects. Below this transition temperature, the very low concentration of intrinsic charge carriers has negligible influence on the total conductivity. A second bend in the Arrhenius plot to higher activation energy from stage II to stage III should occur at lower temperatures, where defect clustering prevails. Supposing association energies within the range of 0·2–0·5 eV, Nowick & Park[20] have calculated the temperature at which half of the total extrinsic oxygen vacancies will be free. They assumed this 'break point temperature' between stages II and III, which varies in calcia-stabilized zirconia between 800 K and the melting point, to be the limit of the associate behavior of oxygen vacancies.

However, in a recent AC impedance spectroscopy study on yttria-doped zirconias,[21] it could be ascertained that the decrease in intragrain ionic conductivity with increasing Y_2O_3 doping is caused by the reduction of oxygen vacancy mobilities. The relaxation frequency of ionic conductivity attributed to the vacancy migration in the lattice revealed the same value of the activation energy as that of the intragrain bulk ionic conductivity itself. Moreover, the calculated concentration of charge carriers remained approximately constant over the whole temperature range investigated (300–1270 K). On the other hand, it has also been shown that the total conductivity of polycrystalline yttria-stabilized zirconia ceramics at low temperatures (stage III) is diminished by the grain boundary impurity phase, which requires a higher activation energy for conduction.[22] Various authors have confirmed this finding, that in polycrystalline ceramics at low temperatures the total resistivity is controlled by the thermally activated process of charge transport through the grain boundaries.[23–26] This interfacial blocking effect of grain boundaries disappears at higher temperatures (stage II), where the electrical properties of grains and grain boundaries converge, approaching the values for single crystals.

Very recently, Weller & Schubert[12] have also found that both the activation energy of bulk ionic conductivity and that of dielectric relaxation are equal within the limits of experimental scatter. However, from the concept of associated charge carriers in stage III,[9,19–20] they questioned the validity of all present values of intragrain bulk conductivities and their activation energies in ceramic materials, obtained by impedance spectroscopy. They presume that the first, high-frequency semicircle in the complex plane of AC impedance diagrams corresponds to a polarization current due to the reorientation of associated dipoles only, instead of bulk conductivity, and that the second semicircle, which has, up to now, been attributed to grain boundary effects, is caused by the intragrain migration of ionic charge carriers. They suggest a revision of the interpretation of the experimental method of AC impedance spectroscopy, introduced by Koops[24] and Bauerle,[25] which is now widely used to characterize the temperature dependence of particular conductivity contributions related to grains, grain boundaries and electrodes.[26]

The present work has been carried out in order to determine the temperature dependence of the relaxation process of the intragrain ionic conductivity in $Zr_{0.85}Ca_{0.15}O_{1.85}$ which is related to the migration of charge carriers in the crystal lattice. A comparison of the calculated activation energy of the charge carrier mobility with that of the bulk ionic conductivity will reveal whether the concentration of 'free' oxygen vacancies changes with temperature or not. Moreover, the volume concentration of mobile charge carriers can be determined. The aim of this work is to study the dynamic transport properties of charge carriers responsible for the high ionic conductivity in this material in order to correlate this behavior with any of the models proposed in the literature. To eliminate the influence of microstructural defects, especially grain boundaries, a gem-quality single crystal of calcia-stabilized zirconia was used.

2 Experimental

A transparent, clear, single crystal of calcia-stabilized zirconia grown by the skull melting method ('Djevalite') was provided by H. Djevahirdijan S.A., CH-1870 Monthey, Switzerland. Chemical analysis of this crystal by EDX revealed that the composition corresponded to $Zr_{0.85}Ca_{0.15}O_{1.85}$. The lattice constant a of the cubic phase having this composition equals 0·513 nm at 290 K and 0·520 nm at 1550 K.[7] The electrical measurements between 450 and 1200 K in air were carried out on a polished specimen $10 \times 5 \times 2\,mm^3$ over a broad frequency range from DC to 300 MHz, using both the four point DC method and the two-point AC technique. Platinum electrodes were painted on the specimen by applying a conductive platinum paste (Demetron 308A) and sintered onto the surface at 1200 K for 4 h. For the complex AC impedance measurements in the frequency range 20–10^6 Hz a PC-controlled precision LCR-meter with correction capability cancelling errors due to the test fixture and test leads, HP 4284A, was used. To minimize the stray capacitance of the test leads, they were kept as short as possible. The shields of the measurement terminals were grounded. Using standard resistors and capacitors whose impedance is close to that of the sample, all measurements were referenced to these

standards. The electrical conductivity was calculated by means of the equation $\sigma = L/(SR)$, where R = the resistance, L = the distance between the electrodes of the measuring cell and S = the area of the electrodes. The temperature was controlled to $\pm 2°C$.

The cell impedance of the single crystal specimen originates from the contribution of the electrolyte material itself and from the electrode/electrolyte interfaces. A simplified equivalent circuit consists of two resistors in series, each shunted in parallel by a capacitor. The first parallel RC-element represents the bulk electrolyte material, the second one the resistance and capacitance of the electrodes. Since the time constants, $\tau = RC$, of both these elements differ by orders of magnitude, at sufficiently high frequencies the second RC-element is shorted and only the impedance of the bulk material is measured.

The Cole–Cole diagram uses the dependence of the imaginary (Z'') and of the real (Z') parts of the complex impedance on the AC frequency, $f = \omega/2\pi$, according to the equations

$$Z'' = -|Z| \sin \Theta$$

and

$$Z' = |Z| \cos \Theta$$

where $|Z|$ = the modulus of impedance and Θ = the angle between the electrical current and voltage. The complex impedance data, $Z = U/I = Z' - iZ''$, are displayed in the complex impedance plane Z'–Z''. In this plane two distinct semicircles can be seen, which correspond to both RC-elements. There is a distinct minimum in the imaginary part Z'' between the first semicircle attributed to the bulk material and the second semicircle attributed to the electrodes; the value of the real part of the complex impedance Z' at this minimum corresponds to the individual resistance of the bulk material. Moreover, from the maximum of Z'' at the top of each semicircle, the relaxation frequency of the corresponding process can be determined ($\omega_R = 1/\tau = 2\pi \cdot f_R$).

At high frequencies, a galvanostatic pulse technique (after Yokota[27]) was employed for the determination of relaxation frequencies by imposing the current and measuring the potential difference over the sample. Figure 1 shows the measuring arrangement for this method. Rectangular square-wave voltage pulses with amplitude $U = 300$ mV from the pulse generator (EGS-2230) force current pulses through the single crystal sample. The voltage drop across the resistor, R_1, which corresponds to the passing current is analyzed at the first input, U_1, of the two-channel oscilloscope (Le Croy 9450A, 300 MHz). Voltage pulses between the inner electrodes of the four-point connected sample are simultaneously observed at the other input

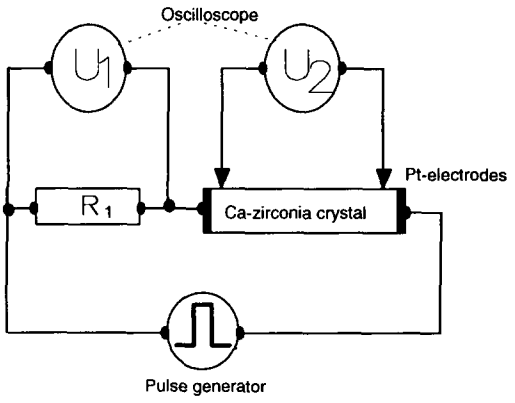

Fig. 1. Measuring arrangement of the pulse method (U_1, channel 1; U_2, channel 2).

of the oscilloscope, U_2. Figure 2 shows the shape of these voltage pulses, U_2, measured on the $Zr_{0.85}Ca_{0.15}O_{1.85}$ single crystal.

The dielectric response results from the short-range motion of charge carriers under the influence of an applied electric field. A measure of the charging time of a capacitor is the time constant τ. On switching the current, charged oxygen vacancies are forced to jump to the adjacent anion sites in the direction of the applied electric field. This migration of charge carriers by hopping results in a localized displacement of the electric dipoles represented by pairs of $V_{\ddot{O}}$ oxygen vacancies with oppositely charged $Ca_{Zr''}$ ions. The time constant of the response of the relaxational intragrain RC-circuit due to the resulting diffusional polarization is expressed by $\tau = RC$. This means that the formation of the diffusional polarization is delayed by the relaxation phenomena. The relaxation frequency corresponds to the time rate at which the stationary polarization is attained. When the current is switched off, the decay process of the polarization reveals the same relaxational behavior.

The time constant τ for the formation and decay processes of the diffusional polarization, which is related to the jump frequency of the charge carriers which may be trapped by defect cations, can be easily followed on the voltage pulses U_2 (see Fig. 2). It corresponds to the time at which 69·3% of the total charging of the final state ($t \gg \tau$) with potential value U_2 is achieved ($\approx 0{\cdot}7U_2$). The charging process is associated with the storage of electric charge by the diffusional polarization resulting from the

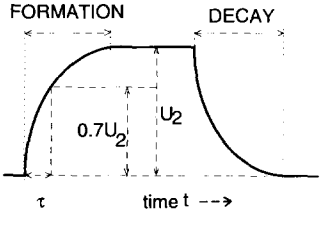

Fig. 2. Voltage pulses between the inner electrodes of a $Zr_{0.85}Ca_{0.15}O_{1.85}$ single crystal specimen.

hopping of charged oxygen vacancies in a direction parallel to the applied field. The agreement between AC impedance measurements and the pulse method is very satisfactory. From the oscilloscope, the relaxation frequency $\omega_R \approx \tau^{-1}$ in the bulk material can be estimated even at high temperatures, at which the relaxation dispersion occurs at frequencies lying above the frequency range of the LCR-bridge.

3 Results

The frequency dependence of the ionic conductivity of $Zr_{0.85}Ca_{0.15}O_{1.85}$ single crystals at different temperatures is shown in Fig. 3. The relaxation dispersion regions of the ionic conductivity σ (Fig. 3) shift towards higher frequencies with increasing temperature. This indicates that these dispersions are thermally activated. At low temperatures the intragrain relaxation process in the zirconia lattice can be seen at high frequencies, but the electrode effects are too slow to be detected. In the temperature range from 673 K to 873 K both dispersions of the electrodes and of the bulk material are observed in the frequency range between 20 and 10^6 Hz. At higher temperatures the effect of the intragrain processes disappears at the higher frequencies and only the dispersion due to the electrode effects can be seen in the middle of the frequency window.

The observed relaxation dispersions can be analyzed using the frequency dependencies of the AC impedance in the complex plane (Cole–Cole diagram). As an example, the complex impedance plot of $Zr_{0.85}Ca_{0.15}O_{1.85}$ single crystal at 666 K is shown in Fig. 4. Below about 600 K only one semicircle appears in the complex AC impedance plane, while at high temperatures a second semicircle due to the electrode processes can be observed. An almost perfect shape of the first semicircle indicates that only a very narrow distribution of relaxation frequencies exist. The real part of the impedance Z', determined from the extrapolated intersection of the

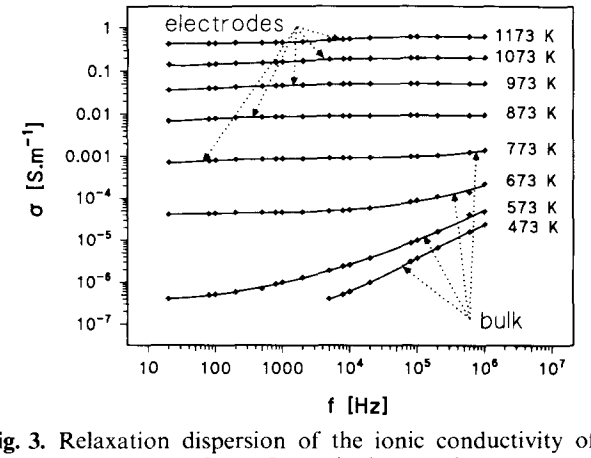

Fig. 3. Relaxation dispersion of the ionic conductivity of a $Zr_{0.85}Ca_{0.15}O_{1.85}$ single crystal.

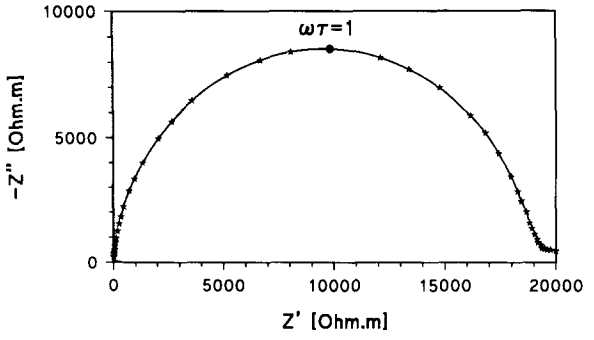

Fig. 4. Complex impedance diagram of a $Zr_{0.85}Ca_{0.15}O_{1.85}$ single crystal at $T = 666$ K.

first semicircle and abscissa, corresponds to the resistivity of bulk material. The angular frequency at the top of the semicircle, at which the highest migration losses due to oscillating oxygen vacancies occur, is the relaxation frequency ω_R of the electrical response of the corresponding RC-circuit. This relaxation frequency at the highest Z'' value can be obtained from the relation $\omega_R \tau = 1$, where $\omega_R = 2\pi f_R$ is the angular frequency, f_R the corresponding frequency of the applied AC field and $\tau = RC = 1/\omega_R$ the time constant of the relaxation circuit.

The temperature dependence of the intragrain bulk ionic conductivity as determined from AC impedance spectroscopy is shown as two Arrhenius plots, $\log \sigma$ against $1/T$ and $\log \sigma T$ against $1/T$, in Fig. 5. No curvature of the Arrhenius plots can be observed. The slope of the straight line of the plot corresponds to the activation energy of the ionic conductivity. There is a noticeable difference of about 0·06 eV between the activation energy estimated from the $\log \sigma$ versus $1/T$ slope (ΔE_σ) and that from $\log \sigma T$ versus $1/T$ plot ($\Delta E_{\sigma T}$). Since $\sigma = A/T \exp(-\Delta E/kT)$, the actual activation energy of ionic conductivity corresponds to $\Delta E_{\sigma T}$, although the lower value of ΔE_σ is often given for the activation energy in the literature. The bulk electrical conductivity of the $Zr_{0.85}Ca_{0.15}O_{1.85}$ single crystal amounts to $1{\cdot}58 \times 10^{-4}$ S m^{-1} at 700 K, changing exponentially with temperature with an activation energy $\Delta E_\sigma = 1{\cdot}26$ eV and $\Delta E_{\sigma T} = 1{\cdot}32$ eV, respectively. This is in agreement with

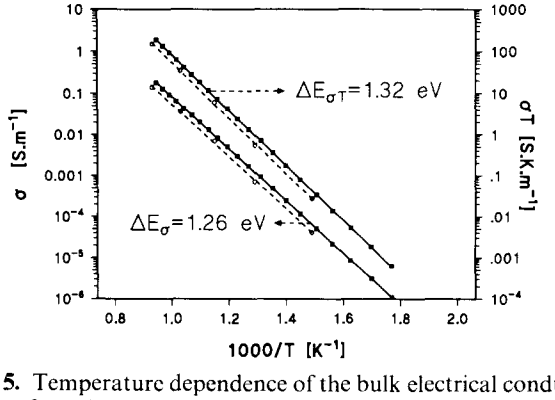

Fig. 5. Temperature dependence of the bulk electrical conductivity of a $Zr_{0.85}Ca_{0.15}O_{1.85}$ single crystal (AC impedance spectroscopy). ○, Kingery *et al.*,[2] ■, this study.

Table 1. Ionic conductivity of $Zr_{0.85}Ca_{0.15}O_{1.85}$ single crystals

Temperature, T (K)	*Ionic conductivity, σ (Sm^{-1})*	*Relaxation frequency, ω_R ($rad\,s^{-1}$)*
565	1.095×10^{-6}	9.42×10^{2}
589	3.123×10^{-6}	3.14×10^{3}
615	8.534×10^{-6}	9.42×10^{3}
640	2.146×10^{-5}	2.51×10^{4}
664	5.106×10^{-5}	5.65×10^{4}
690	1.142×10^{-4}	1.26×10^{5}
715	2.437×10^{-4}	2.51×10^{5}
739	4.855×10^{-4}	5.03×10^{5}
763	9.268×10^{-4}	9.42×10^{5}
789	1.693×10^{-3}	1.76×10^{6}
814	2.987×10^{-3}	3.14×10^{6}
837	5.083×10^{-3}	5.03×10^{6}
862	8.263×10^{-3}	7.54×10^{6}
886	1.312×10^{-2}	—
911	2.035×10^{-2}	—
935	3.025×10^{-2}	—
960	4.364×10^{-2}	—
984	6.396×10^{-2}	—
1009	9.262×10^{-2}	—
1033	1.283×10^{-1}	—
1058	1.793×10^{-1}	—

results reported in the literature.[1,2] To make a comparison, the σ values of the total DC conductivity obtained by Kingery *et al.*[2] on polycrystalline $Zr_{0.85}Ca_{0.15}O_{1.85}$ ceramic specimens are also shown in Fig. 5.

From the results of complex impedance measurements summarized in Table 1, the temperature dependence of the relaxation frequency of processes within the single crystal (ω_R) can be determined. The relaxation frequency of the bulk ionic conductivity due to the migration of oxygen vacancies changes exponentially with temperature with the activation energy $\Delta E_{\omega R} = 1.26\,eV$ (see Fig. 6).

4 Discussion

The ionic conductivity in calcia-doped zirconia, which involves the long-range migration of extrinsic

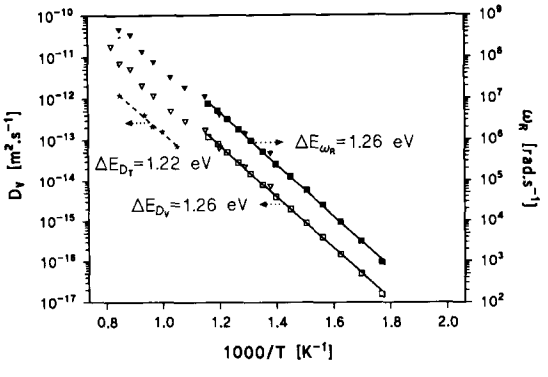

Fig. 6. Temperature dependence of the relaxation frequency ω_R and the diffusion coefficient D_V of oxygen vacancies in a $Zr_{0.85}Ca_{0.15}O_{1.85}$ single crystal. ★, D_T from Kingery *et al.*;[2] □, ■, AC impedance spectroscopy; ▽, ▼, pulse method.

oxygen vacancies, is expressed as the product of the volume concentration n (m^{-3}), the electrical mobility μ ($m^2\,V^{-1}\,s^{-1}$), and the electric charge q (As) ($q = 2e$, $e = 1.6 \times 10^{-19}$ As) of mobile oxygen vacancies:

$$\sigma = n\mu q = n\mu 2e \tag{1}$$

Both the charge carrier concentration and their mobility are included in this relation. Furthermore, both these parameters could be thermally activated if an association of oxygen vacancies in defect complexes occurs. From conductivity measurements alone it is therefore not possible to resolve whether the oxygen vacancy concentration changes with temperature or not. The temperature dependence of the ionic conductivity can be written as:

$$\begin{aligned}\sigma &= (A/kT)\exp(-\Delta E_{\sigma T}/kT) \\ &= [n_0 \exp(-\Delta E_n/kT)] \\ &\quad \times [(C/kT)\exp(-\Delta E_{\mu T}/kT)]q\end{aligned} \tag{2}$$

where ΔE_n means the activation energy of the 'free' oxygen vacancy formation and $\Delta E_{\mu T}$ is the activation energy for their migration. The first term describes the temperature dependence of the concentration of mobile charge carriers, the second term characterizes their mobility within the material. Accordingly, the total activation energy for the bulk ionic conduction $\Delta E_{\sigma T}$ is the sum of both activation energy contributions:

$$\Delta E_{\sigma T} = \Delta E_n + \Delta E_{\mu T} \tag{3}$$

The activation energy ΔE_n for the formation of 'free' oxygen vacancies due to the dissociation of the assumed defect-pairs corresponds to the half value of the free enthalpy ΔG_A of the association reaction ($\Delta E_n = \Delta G_A/2$).

According to the Nernst–Einstein relation, the diffusion constant of oxygen vacancies D_V is directly proportional to the mobility μ:

$$\mu = q \cdot D_V/kT \tag{4}$$

where $D_V = D_0 \exp(-\Delta E_{D_V}/kT)$. That means that the activation energies of vacancy diffusion and migration should be equal:

$$\Delta E_{D_V} = \Delta E_{\mu T} \tag{5}$$

The ionic conductivity, σ, is related to the lattice diffusion coefficient of mobile oxygen vacancies, D_V, by the Nernst–Einstein equation (4):

$$D_V = kT\sigma/(nz^2e^2) \tag{6}$$

where n = concentration of mobile oxygen vacancies per unit volume, $k = 8.617 \times 10^{-5}\,eV\,K^{-1}$ = the Boltzmann's constant, $e = 1.6 \times 10^{-19}$ As = the elementary electronic charge, z = the valence of the charged vacancies and D_V = the lattice diffusion coefficient for oxygen vacancies. Using relation (1)

for the migration of charge carriers, $\mu = \sigma/(nze)$, the temperature dependence for the electrical mobility of oxygen vacancies ($z = 2$), can be calculated according to:

$$\mu = D_V 2e/kT \tag{7}$$

As pointed out in the introduction, the dielectric response to the alternating electric field applied across the material occurs as a result of the short-range motion (hopping) of charged oxygen vacancies between anion sites. This temperature-activated diffusional polarization mechanism involves ionic migration of the same mobile oxygen vacancies which contribute to the bulk DC conductivity due to the long-range migration. According to the simple random walk model of thermally activated jumps, the dispersion of the frequency dependence of the ionic conductivity can be associated with the hopping of charged oxygen vacancies over the nonequivalent energy barriers.[17] The relaxation time of this process reflects the statistical distribution of jump frequencies. Assuming the motion of oxygen vacancies to consist of discrete jumps over the length L, the diffusion coefficient for cubic site symmetry is related to the relaxation frequency ω_R by the expression:

$$D_V = d^2\omega_R\gamma/6 \tag{8}$$

where d^2 is the mean square distance between the oxygen sites in the elementary cell of the $Zr_{0.85}Ca_{0.15}O_{1.85}$ single crystal, γ is the correlation factor which depends on the definition and probability population of jump vectors, and $\frac{1}{6}$ is the geometric factor for three-dimensional motion in a cubic lattice. The parameter d in eqn (4) actually shows the mean jump distance of oxygen ions which is limited to jumps to nearest and next-nearest neighbouring sites in the range $a/2$ along the [100] direction to $a\sqrt{2}/2$ along the [110] direction. For single crystals of $(ZrO_2)_{0.88}$–$(Y_2O_3)_{0.12}$ the product of the mean square displacement d^2 and the correlation factor γ, $d^2\gamma = 0.35a^2$ was derived, which means that the probability of the [100] jump direction is about 60%.[17]

The temperature dependence of the relaxation frequency is given by:

$$\omega_R = \omega_0 \exp(-\Delta E\omega_R/kT) \tag{9}$$

where ω_0 is related to the Debye limiting infrared phonon frequency of the lattice vibrations[28] which is in the range 10^{12}–10^{13} Hz. It can be seen from relations (5), (8) and (9) that $\Delta\omega_R = \Delta E_{D_V} = \Delta E_{\mu T}$.

From the experimental data of the measurements of $\omega_R(T)$ after both the pulse and the complex AC impedance method it is possible to calculate the temperature dependence of the diffusion coefficient by means of eqn (8). For the calculation of $d^2\gamma$ according to Abelard & Baumard[17] the structural parameter a from Ref. 7 has been used ($a \cong 0.516$ nm at 800 K).[7] The experimental results for the temperature dependence of the relaxation frequency, $\omega_R(T)$, are shown together with the calculated diffusion coefficients, $D_V(T)$, in Fig. 6.

At $T = 800$ K the diffusion coefficient D_V is 3.49×10^{-15} m^2 s^{-1}. It changes exponentially with temperature with the activation energy $\Delta E_{D_V} = 1.26$ eV. As seen from Fig. 6, the values of ΔE_{D_V} and $D_V(T)$ for $Zr_{0.85}Ca_{0.15}O_{1.85}$ single crystal (Table 2) are a little higher than the values of the tracer diffusion coefficient D_T determined on $Zr_{0.85}Ca_{0.15}O_{1.85}$ polycrystals by Kingery *et al.*[2] This is in good agreement with the later D_V data reported in the literature.[29] The tracer diffusion coefficient D_T is equal to the diffusion coefficient of oxygen vacancies D_V times the site fraction of the vacant lattice sites $[V_{\ddot{O}}]$: $D_T = D_V[V_{\ddot{O}}]$. For 15 mol% CaO-stabilized zirconia $[V_{\ddot{O}}] = 0.15/2 = 0.075$.

Combining eqns (3) and (4), the mobility of the ionic charge carriers associated with the diffusion process can be calculated from the equation:

$$\mu = d^2ze\omega_R\gamma/6kT \tag{10}$$

Table 2. Diffusion coefficient and mobility of oxygen vacancies in $Zr_{0.85}Ca_{0.15}O_{1.85}$ single crystals

Temperature, T (*K*)	*Diffusion coefficient, D_V* ($m^2 s^{-1}$)	*Mobility, μ* ($m^{-2} V^{-1} s^{-1}$)	*Concentration, n* ($\times 10 m^{-3}$)
565	1.46×10^{-17}	5.99×10^{-16}	5.71
589	4.88×10^{-17}	1.92×10^{-15}	5.08
615	1.46×10^{-16}	5.50×10^{-15}	4.85
640	3.90×10^{-16}	1.41×10^{-14}	4.76
664	8.78×10^{-16}	3.07×10^{-14}	5.20
690	1.96×10^{-15}	6.59×10^{-14}	5.42
715	3.90×10^{-15}	1.26×10^{-13}	6.04
739	7.81×10^{-15}	2.45×10^{-13}	6.19
763	1.46×10^{-14}	4.44×10^{-13}	6.52
789	2.73×10^{-14}	8.02×10^{-13}	6.60
814	4.88×10^{-14}	1.39×10^{-12}	6.72
837	7.81×10^{-14}	2.16×10^{-12}	7.35
862	1.17×10^{-13}	3.15×10^{-12}	8.20

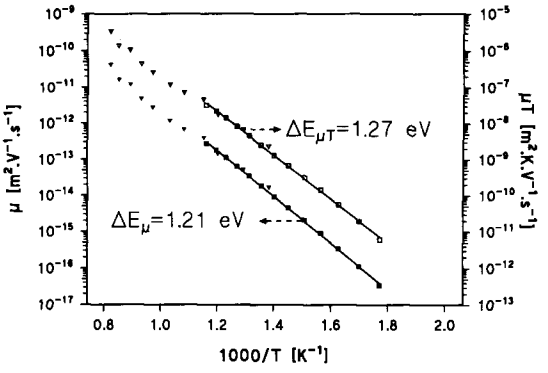

Fig. 7. Temperature dependence of the mobility μ of oxygen vacancies in a $Zr_{0.85}Ca_{0.15}O_{1.85}$ single crystal. □, ■, AC impedance spectroscopy; ▽, ▼, pulse method.

The Arrhenius plot of the temperature dependence of oxygen vacancy mobilities is shown in Fig. 7. At $T = 800\,K$ the ionic mobility μ amounts to $1{\cdot}02 \times 10^{-12}\,m^2\,V^{-1}\,s^{-1}$. The activation energy of the mobility $\Delta E_{\mu T} = 1{\cdot}26\,eV$ is identical both to ΔE_{D_V} and $\Delta E\omega_R$. The calculated values of the diffusion coefficient D_V and the charge carriers mobility at various temperatures are summarized in Table 2.

When ZrO_2 is stabilized with CaO, the addition of each Ca atom generates one oxygen vacancy. The defect structure written in Kröger–Vink notation can be described by the following equation:

$$CaO \xrightarrow{ZrO_2} Ca''_{Zr} + V_{\ddot{O}} + O_O$$

The volume concentration of all extrinsic oxygen vacancies resulting from this reaction, n_0, can be calculated according to Hohnke[9] by employing the equation:

$$n_0 = 4x/a^3 \qquad (11)$$

where a is the lattice parameter of the stabilized zirconia cubic cell containing four $Zr_{1-x}Ca_xO_{2-x}$ formula units and x is the number of oxygen vacancies per one formula unit corresponding to the mole fraction of CaO. For $Zr_{0.85}Ca_{0.15}O_{1.85}$ ($x = 0{\cdot}15$), $n_0 = 4{\cdot}37 \times 10^{27}\,m^{-3}$ is obtained.

The actual number of mobile, charge-carrying oxygen vacancies available in the $Zr_{0.85}Ca_{0.15}O_{1.85}$ single crystal, n, can be easily determined from the experimental values of both the ionic conductivity, σ, and the relaxation frequency, ω_R, combining eqns (1) and (10). The amount of intrinsic oxygen vacancies produced by thermal disorder can be neglected because of the very high activation energy of the formation of intrinsic defects.[8] The total concentration of extrinsic oxygen vacancies, n_0, is given by eqn (11).

Table 2 shows that at all temperatures within the investigated range the calculated concentration of mobile oxygen vacancies, n, remains approximately equal to the value for the concentration of all extrinsic vacancies created by doping:

$$n \cong n_0 = 4{\cdot}37 \times 10^{27}\,m^{-3}$$

Therefore, the presumed association of stabilizer–vacancy defect pairs does not influence the concentration of the mobile charge carriers which are responsible for the electrical conductivity, but only reduces their electrical mobility, μ.

The small difference between activation energies of the ionic conductivity $\Delta E_{\sigma T}$ and of the migration of ionic charge carriers $\Delta E_{\mu T}$, which amounts to about 0·06 eV, is within the accuracy limit of the measurements of $\pm 5\%$. This coincidence of activation energies for the charge transport process proves that the temperature dependence of ionic conductivity, $\sigma(T)$, is determined only by the thermally activated mobility of oxygen vacancies, $\mu(T)$, while the concentration of charge carriers remains constant. The calculated values for $\sigma(T)$ according to eqn (1), using mobility data derived by means of eqn (10), show a very good agreement with experimentally determined values for the ionic conductivity σ of the $Zr_{0.85}Ca_{0.15}O_{1.85}$ single crystal.

From the experimental data the following three conclusions can be drawn:

(a) The concentration of charge-carrying oxygen vacancies in $Zr_{0.85}Ca_{0.15}O_{1.85}$ does not change with temperature.
(b) The activation energies for both the ionic conductivity and the mobility of oxygen vacancies in $Zr_{0.85}Ca_{0.15}O_{1.85}$ are equal.
(c) There is no curvature in the Arrhenius plot of the bulk ionic conductivity of $Zr_{0.85}Ca_{0.15}O_{1.85}$ single crystals between 450 and 1200 K if electrode effects are properly separated.

5 Conclusions

Complex impedance spectroscopy and the dynamic pulse technique provide, through the determination of the relaxation frequency of ionic conduction, a simple tool for studying the dynamic nature of charge transport processes in solid electrolytes. In the present work information on the dynamics of the oxygen vacancy motion in a $Zr_{0.85}Ca_{0.15}O_{1.85}$ single crystal has been obtained in the frequency range 20–10^8 Hz. The dielectric relaxation arises from the short-range motion of charged oxygen vacancies which oscillate between anion sites parallel to the electric field. The determination of the relaxation frequency, $\omega_R = 2\pi f_R$, corresponding to a mean jump rate of oxygen vacancies, $1/\tau$, allows their mobility as well as the diffusion coefficient to be

calculated. A very narrow distribution of relaxation times shows that mainly one polarization mechanism exists. Since the activation energies of the ionic conductivity, relaxation frequency and charge carrier mobility were found to be equal, the concentration of hopping charge carriers in calcia-stabilized zirconia is invariant with temperature. Moreover, the volume concentration of mobile charge carriers calculated from the values of the ionic conductivity and the relaxation frequency corresponds to the concentration of all extrinsic oxygen vacancies created by doping. It can be concluded that in the temperature range investigated (450–1200 K) there is no difference between 'free' and 'immobile' charge carriers but all oxygen vacancies take part in the conduction process. A low-temperature bend in the Arrhenius conductivity plot represents no transition from the 'associated' to the 'dissociated' range but is caused by an additional resistance being in series with the bulk material, which blocks the transport of charge carriers at low temperatures. Such additional serial resistance to the bulk material may originate from all kinds of interfacial defects lying transverse to the current path, namely grain boundaries, domains, segregations, cracks and electrode surfaces. Hence this serial element exhibits a higher activation energy for conduction than the bulk material itself, the blocking effect vanishes at high temperatures.

The temperature dependence of the total ionic conductivity of solid electrolytes can be explained by a simple equivalent electrical circuit consisting both of parallel and series combinations of temperature-dependent RC-elements. The RC-element controlling the overall process will determine the total conductivity of the whole circuit in the corresponding temperature region.

Acknowledgements

This work was financially supported by the Swiss Federal Office of Energy. The authors express their gratitude to the firm H. Djevahirdijan S.A. for the kind gift of the $Zr_{0.85}Ca_{0.15}O_{1.85}$ single crystal and thank Prof. G. Bayer and Prof. P. D. Ownby for helpful discussions and reviewing the manuscript.

References

1. Kiukkola, K. & Wagner, C., Measurements on galvanic cells involving solid electrolytes. *J. Electrochem. Soc.*, **104** (1957) 379–87.
2. Kingery, W. D., Pappis, J., Doty, M. E. & Hill, D. C., Oxygen ion mobility in cubic $Zr_{0.85}Ca_{0.15}O_{1.85}$. *J. Am. Ceram. Soc.*, **42** (1959) 393–8.
3. Stricker, D. W. & Carlson, W. G., Ionic conductivity of cubic solid solutions in the system CaO–Y_2O_3–ZrO_2. *J. Am. Ceram. Soc.*, **47** (1964) 122–7.
4. Stricker, D. W. & Carlson, W. G., Electrical conductivity in the ZrO_2–rich region of several M_2O_3–ZrO_2 systems. *J. Am. Ceram. Soc.*, **48** (1965) 286–9.
5. Bonanos, N., Slotwinski, R. K., Steele, B. C. H. & Butler, E. P., Electrical conductivity/microstructural relationships in aged CaO and CaO + MgO partially stabilized zirconia. *J. Mater. Sci.*, **19** (1984) 785–93.
6. Aldebert, P. & Travers, J-P., Structure and ionic mobility of zirconia at high temperature. *J. Am. Ceram. Soc.*, **68** (1985) 34–40.
7. Neder, R. B., Frey, F. & Schulz, H., Defect structure of zirconia ($Zr_{0.85}Ca_{0.15}O_{1.85}$) at 290 and 1550 K. *Acta Cryst.*, **A46** (1990) 799–809.
8. Dwivedi, A. & Cormack, A. N., A computer simulation study of the defect structure of calcia-stabilized zirconia. *Phil. Mag.*, **A61** (1990) 1–22.
9. Hohnke, D. K., Ionic conduction in doped zirconia. In *Fast Ion Transport in Solids*, ed. P. Vaskista, J. N. Mundy & G. K. Shenoy. Elsevier, North-Holland, Inc., New York, 1979, pp. 669–72.
10. Nakamura, A. & Wagner, J. B., Defect structure, ionic conductivity, and diffusion in yttria stabilized zirconia and related oxide electrolytes with fluorite structure. *J. Electrochem. Soc.*, **133** (1986) 1542–8.
11. Weller, M. & Schubert, H., Internal friction, dielectric loss, and ionic conductivity of tetragonal ZrO_2–3%Y_2O_3 (Y-TZP). *J. Am. Ceram. Soc.*, **69** (1986) 573–7.
12. Weller, M. & Schubert, H., Defects in ZrO_2–Y_2O_3 studied by mechanical and dielectric loss measurements. In *Solid State Ionics*, ed. M. Balkanski, T. Takahaski & H. L. Tuller. Elsevier, Amsterdam, 1992, pp. 569–74.
13. Subbarao, E. C. & Ramakrishnan, T. V., Ionic conductivity of highly defective oxides. In *Fast Ion Transport in Solids*, ed. P. Vashista, J. N. Mundy & G. K. Shenoy. Elsevier, North-Holland Inc., New York, 1979, pp. 653–6.
14. Badwal, S. P. S., Electrical conductivity of single crystal and polycrystalline yttria-stabilized zirconia. *J. Mater. Sci.*, **19** (1984) 1767–76.
15. Badwal, S. P. S., Comment on low-temperature ionic conductivity of 9·4 mol% yttria-stabilized zirconia single crystals. *J. Am. Ceram. Soc.*, **73** (1990) 3718–9.
16. Catlow, C. R. A., Defect clustering in nonstoichiometric oxides. In *Nonstoichiometric Oxides*, ed. O. T. Sorensen. Academic Press, New York, 1981, pp. 61–98.
17. Abelard, P. & Baumard, J. F., Study of the DC and AC electrical properties of an yttria-stabilized zirconia single crystal $[(ZrO_2)_{0.88}$–$(Y_2O_3)_{0.12}]$. *Phys. Rev. (B)*, **26** (1982) 1005–17.
18. Ananthapadmanabhan, P. V., Venkatramani, N., Rohagi, V. K., Momin, A. C. & Venkateswarlu, K. S., Structure and ionic conductivity of solid solutions in the system $0{\cdot}9[ZrO_2]_{1-x}[CeO_2]_x$–$0{\cdot}1[Y_2O_3]$. *J. Eur. Ceram. Soc.*, **6** (1990) 111–17.
19. Nowick, A. S., Wang, D. Y., Park, D. S. & Griffith, J., Oxygen-ion conductivity and defect structure of CeO_2 doped with CaO and Y_2O_3. In *Fast Ion Transport in Solids*, ed. P. Vashista, J. N. Mundy & G. K. Shenoy. Elsevier, North-Holland Inc., New York, 1979, pp. 673–9.
20. Nowick, A. S. & Park, D. S., Fluorite-type oxygen conductors. In *Superionic Conductors*, ed. G. Mahan & W. Roth. Plenum Press, New York, 1976, pp. 395–412.
21. Orliukas, A., Sasaki, K., Bohac, P. & Gauckler, J., Ionic conductivity of ZrO_2–Y_2O_3 prepared from ultrafine coprecipitated powders. In *Proceedings 2nd Intl. Symp. Solid Oxide Fuel Cells*, The European Communities, Athens, 2–5 July 1991, pp. 377–85.
22. Orliukas, A., Heeb, B., Michel, B., Sasaki, K., Bohac, P. & Gauckler, L., The effect of intergranular glass phase on the electrical properties of Y-TZP. In *Proceedings Eur. Ceram. Soc. 2nd Conference*, Augsburg, 11–14 September 1991.
23. Kleitz, M., Bernard, H., Fernandez, E. & Schouler, E.,

Impedance spectroscopy and electrical resistance measurements on stabilized zirconia. In *Advances in Ceramics*, Vol. 3, ed. A. H. Heuer & L. W. Hobbs. American Ceramic Society, Inc., Columbus, Ohio, 1981, pp. 310–36.
24. Koops, C. G., On the dispersion of resistivity and dielectric constant of some semiconductors at audiofrequencies. *Phys. Rev.*, **83** (1951) 121–4.
25. Bauerle, J. E., Study of solid electrolyte polarization by a complex admittance method. *J. Phys. Chem. Solids*, **30** (1969) 2657–70.
26. Verkerk, M. J., Winnubst, A. J. A. & Burggraaf, A. J., Effect of impurities on sintering and conductivity of yttria-stabilized zirconia. *J. Mater. Sci.*, **17** (1982) 3113–22.
27. Yokota, I., On the theory of mixed conduction with special reference to the conduction in silver sulfide group semiconductors. *J. Phys. Soc. Japan*, **16** (1961) 2213–23.
28. Nevitt, M. V., Heat capacity of monoclinic zirconia between 2·75 and 350 K. *J. Am. Ceram. Soc.*, **73** (1990) 2502–4.
29. Ando, K. & Oishi, Y., Oxygen self-diffusion in Y_2O_3 and Y_2O_3–ZrO_2 solid solutions. In *Transport in Nonstoichiometric Compounds*, ed. C. Simkovich & V. S. Stubican. Plenum Press, New York, 1985, pp. 203–14.